Acadlore Transactions on Geosciences
https://www.acadlore.com/journals/ATG

AI-Driven Analysis of Rock Fragmentation: The Influence of Explosive Charge Quantity

Nidumukkala Sri Chandrahas[1*], Bhanwar Singh Choudhary[2], Musunuri Sesha Venkataramayya[3], Yewuhalashet Fissha[4], Nageswara Rao Cheepurupalli[5]

[1] Department of Mining Engineering, Malla Reddy Engineering College, 500014 Hyderbad, India
[2] Department of Mining Engineering, IIT(ISM), 826001 Dhanbad, India
[3] Department of Mining Engineering, College of Engineering, Osmania University, 500007 Hyderabad, India
[4] Department of Geosciences, Geo-technology and Materials Engineering for Resources, Graduate School of International Resource Sciences, Akita University, 010-8502 Akita, Japan
[5] Mining Engineering Department, Aksum University, 7080 Aksum, Ethiopia

[*] Correspondence: MNidumukkala Sri Chandrahas (srichandru2009@gmail.com)

Received: 06-05-2024 **Revised:** 07-10-2024 **Accepted:** 07-22-2024

Citation: N. S. Chandrahas, B. S. Choudhary, M. S. Venkataramayya, Y. Fissha, and N. R. Cheepurupalli, "AI-driven analysis of rock fragmentation: The influence of explosive charge quantity," *Acadlore Trans. Geosci.*, vol. 3, no. 3, pp. 123–134, 2024. https://doi.org/10.56578/atg030301.

Abstract: Drilling and blasting are essential operations within the mining industry, playing a critical role in material fragmentation. Despite advancements in various blasting technologies, the process remains a dominant contributor to overall mining costs. Achieving cost efficiency requires the precise configuration of blast design parameters, including explosive charge quantity, to attain desired outcomes in fragmentation, ground vibrations, fly rock, and air over-pressure. This study introduces a novel artificial intelligence (AI)-driven model, XGBoost-PSO-T, which combines eXtreme Gradient Boosting (XGBoost) with Particle Swarm Optimization (PSO) through the integration of the Tri-Weight technique. The PSO-Tri-Weight method optimizes the hyperparameters of the XGBoost model, enhancing its predictive capabilities. The model's performance was evaluated using root mean square error (RMSE) and coefficient of determination (R^2), with the results demonstrating that the XGBoost-PSO-T system outperforms the standard XGBoost approach, achieving an RMSE of 0.657 and an R^2 of 0.922. These findings suggest that the XGBoost-PSO-T model is a valuable tool for predicting fragmentation outcomes and optimizing blast designs in surface mining operations. The implementation of this system is recommended to improve blasting efficiency and reduce operational costs.

Keywords: Rock fragmentation; Explosive charge quantity; Drone; Artificial intelligence

1 Introduction

The rise in civilization and the increasing utilization of minerals have significantly grown in recent times. Minerals and their products are integral to nearly every facet of daily life, and their extraction is facilitated through mining. This process involves various techno-economic aspects and engineering principles to ensure safe and economical extraction.

The primary goal of blasting is to create a muck pile with an optimal rock fragmentation distribution suitable for transportation and beneficiation [1]. Mining operations comprise two major unit operations: drilling and blasting. Competent rock is fragmented using explosives in blasting operations to facilitate easy handling by loading equipment. The key objective of blasting is to achieve optimal fragment size at minimal cost. Enhancing the profitability of mining can be achieved by reducing operational costs, including those related to explosives, loading, and milling. It is widely acknowledged that rock fragmentation significantly impacts loading operations [2, 3].

Achieving optimal fragmentation is crucial for significantly reducing the cost of downstream operations. Target fragmentation varies depending on the equipment used and can differ from mine to mine [4, 5]. The high pressure generated by explosives is responsible for breaking the rock, and this pressure is directly related to the amount of explosive used in the blast hole [6]. The quantity of explosives is significantly influenced by the geo-spatial and blast design parameters of the blasts [7]. Variations in charge length, based on geological rock conditions and decking

length, greatly affect the quantity of explosives needed and the resulting rock blast size [8]. Excessive placement of explosives in weak geological planes leads to unwanted ground vibration and boulder formation due to the waste of shock and gas energy as it attempts to escape [9]. A lack of understanding of rock conditions and the overuse of explosives can result in increased rock fragmentation, negatively impacting mine economics downstream [10].

By technically understanding and selecting the appropriate type and quantity of explosives according to geotechnical rock conditions, good fragmentation can be achieved. In jointed formations, the quantity of explosives plays a crucial role in fragment production [11].

The outcomes of a blast can be either favorable or unfavorable, largely depending on the blast design parameters. These parameters are not fixed and must be adjusted on-site according to the mine's geological conditions. The design should maximize the use of explosive energy while minimizing its wastage. In rocks with closed fissures, the generation of new cracks is unnecessary. Instead, gas pressure from the explosives widens the existing joints, creating multiple loose rocks [12].

Typically, rock fragmentation prediction is carried out using the Kuz-Ram model. This model is based on the Kuznetsov and Rosin-Rammler equations [13], which were modified by Cunningham in 1983 and 1987. It is an empirical fragmentation model that derives the uniformity index used in the Rosin-Rammler equation. The modern version of the Kuz-Ram fragmentation model combines explosive properties, rock properties, and design variables [14, 15]. To implement this empirical method, site-specific constants must be used, which can vary.

Image analysis techniques were used in various numerical experiments on rock fragmentation recently. Technological advancements led to a greater focus on video-based systems and automated machine vision, which are increasingly applied in mine automation processes [16, 17]. The use of drones for capturing rock fragmentation significantly enhanced muck pile analysis in recent years [18].

AI has emerged as a powerful tool with applications across several fields, particularly in addressing technical challenges [19, 20]. Soft computing techniques and optimization algorithms have recently garnered significant attention from the engineering and scientific communities [21, 22], especially for forecasting rock fragmentation [23, 24]. Artificial Neural Networks (ANNs) have been used for predicting rock fragmentation [25]. Similarly, Kuznetsov methods, support vector machines (SVMs), multiple regression (MR) models, and ANNs have been used to forecast rock fragmentation [26]. From an extensive literature review, it can be observed that rock fragmentation prediction and analysis are predominantly conducted using manual methods and empirical equations. While some algorithms have been employed to forecast results in geotechnical and rock blasting fields, there remains a notable gap in the development of robust models that accurately predict rock fragmentation. Most existing models are not sufficiently field-driven, leading to less accurate results.

To address this gap, this study aims to develop a hybrid model that integrates empirical approaches with advanced algorithmic techniques. This hybrid model was designed to enhance prediction accuracy by leveraging both field data and sophisticated analytical methods. By combining these approaches, the study seeks to overcome the limitations of current models and provide a more reliable and accurate framework for predicting rock fragmentation outcomes. The objectives of this study are as follows:

- To understand the influence of blast design parameters on rock fragmentation.
- To execute blasts using both designed and predicted parameters in software.
- To develop a hybrid model based on experimental blast data.
- To predict rock fragmentation using the XGBoost-PSO-T algorithm.

2 Field Study

A field study was conducted at Opencast Mine II, located in the Ramagundam Region III of Singareni Collieries Company Limited, Telangana, as shown in Figure 1. The benches in this mine are 16 meters high, and the rock, which is friable and composed of sandstone, has a specific gravity of 2.4. The blast holes have a diameter of 250 mm and a depth of 17 meters. Site Mixed Emulsion (SME) was used as the explosive. A staggered drilling pattern was adopted, and the firing pattern was a "V" shape, utilizing cast boosters and a NONEL initiation system. The blast design parameters, including burden, spacing, blast hole diameter, length, explosive quantity, and stemming length, were documented.

Figure 1. Opencast Mine at RGIII, Ramagundam, SCCL, Telangana

To gather data, a drone was flown over the overburden (OB) bench, capturing photographs with a longitudinal overlap of 70%. The geological condition of the rock mass in the area is isotropic in all directions. Data were collected from 137 blasts, including measurements of burden, spacing, and the quantity of explosives used in each blast.

The DJI MAVIC unmanned aerial vehicle (UAV) was utilized in this investigation to capture high-resolution photographs and videos, recorded in 4K resolution. Weighing 258 grams, the UAV has a flight time of 25 minutes per battery charge. To ensure a successful deployment and mitigate signal issues, calibration was performed before the drone was launched. The UAV captured images of the blast site, as shown in Figure 2.

The UAV was specifically employed to photograph the benches in orthogonal orientations before and after the blast, with the goal of obtaining detailed images of joint planes, joint spacing, and spanning length in the vertical section of the bench. The UAV hovered at an altitude of 100 feet above the bench, covering 75% of the shooting range. The camera was angled between 45 and 60 degrees to focus on both the bench top's corner and the bench floor's edge. This precise capturing direction is critical for generating accurate 3D models used in designing blast patterns that accurately reflect the geo-rock conditions. The bench was divided into three sections: top, bottom, and a combination of crest and toe, which allowed for capturing between 70% and 80% overlap, ensuring thorough documentation.

(a) (b)

Figure 2. (a) Flight calibration; (b) scanning at SCCL mines, Ramagundam

The captured images were processed using Strayos software to analyze the rock mass. Ground control points (GCPs) were marked at the blast site, as illustrated in Figure 3. For each 3D model, four to five GCPs were marked on the surface in a highly visible red color, sequentially numbered. The GCP markers were strategically placed, with a greater number at the outer corners of the site to ensure comprehensive coverage. For areas like muck piles, where placing GCPs is challenging, at least one GCP was attempted for each elevation level. The UAV performed a normal flight while capturing images, taking care to include GCP markers in the frame, avoid distortions, and maintain camera focus. After completing the drone survey, the GCP data was uploaded into the software to create 3D models of the blast benches.

The latitude and longitude of each GCP, following the European Petroleum Survey Group (EPSG) system, were recorded and stored in CSV format with the EPSG code 32,644. This data, along with the drone imagery, was uploaded into Strayos software. The software interface then displayed the GCP positions overlaid on satellite images, allowing for manual confirmation and adjustments. The ground sampling distance considered in this process was 0.49 cm/pixel.

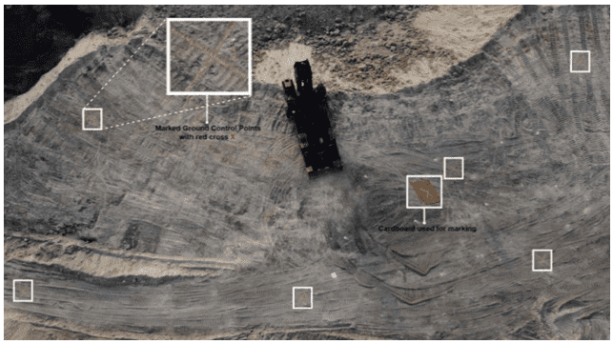

Figure 3. Marked GCP points at site

3 Blast Modeling Using Strayos Software

A 3D AI platform, Strayos software, was used in this study for blast modelling and analysis purposes. Strayos software in blast modeling operates under several key assumptions. It assumes rock mass homogeneity, meaning that rock properties such as density and strength are consistent within certain areas. The software relies on the geometric accuracy of the input data, assuming that the geometry of benches, blast patterns, and boreholes is precisely captured. Consistent explosive properties, such as detonation velocity and energy release, are also assumed to behave predictably under typical conditions. Fragmentation distribution is modeled based on assumed distributions influenced by blast design parameters and rock characteristics. The software assumes even energy distribution from the explosives within the blast volume, and that the burden and spacing are optimal or near-optimal according to industry standards.

Generally, the software needs ten drone photographs to create the 3D model. For this study, photographs were taken with the aid of a drone flying over the bench.

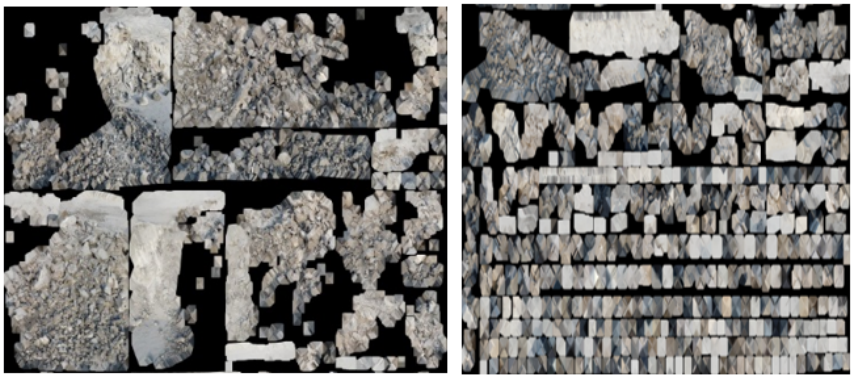

Figure 4. Orthogonal photographs used to create 3D models

The photographs were uploaded into the software, where they were superimposed to create a 3D model of the bench for blast design, as shown in Figure 4. The blast design process involved drilling a series of holes, charging them, and setting timing delays. Predictions were made for the muckpile and fragmentation. Using test data, approximately 30 blast designs were modelled in software similar to those shown in Figure 5 and the mean fragment size for each blast was recorded. The predicted fragment sizes were then compared with the results obtained from the software.

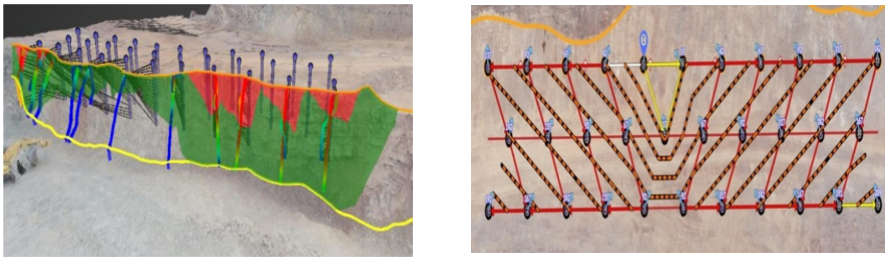

(a) (b)

Figure 5. (a) 3D-burden heat map in Strayos; (b) sequence of initiation and the direction of throw

The figure above illustrates the 3D burden in Strayos software, displaying the distribution of burden along the free face. The green colour represents the sufficient distance between the drill holes and front-row burden for efficient shock energy transmission. The red colour indicates insufficient transmission for rock breakage and displacement. The 3D burden heat map highlights the influence zones along the free face.

The drilled holes were connected with timing delays using a V-pattern, and the hole-to-hole and row-to-row ties were initially connected using 0 delay and 17 ms in software for simulation and prediction, as shown in Figure 5. The figure above depicts the drilling pattern, blast initiation sequence, and throw direction. The holes were loaded with bulk explosives, boosters, and NONEL initiation systems. The resulting mean fragmentation size model, particle sizes and results were indicated in Figure 6, Figure 7, Figure 8, respectively. The mean fragmentation size for each blast model was recorded and used for comparison with the predicted fragmentation size derived from the formula.

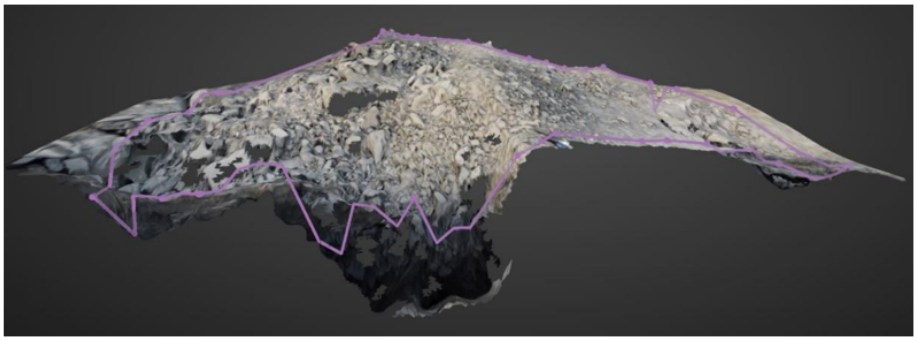

Figure 6. 3D fragmentation model

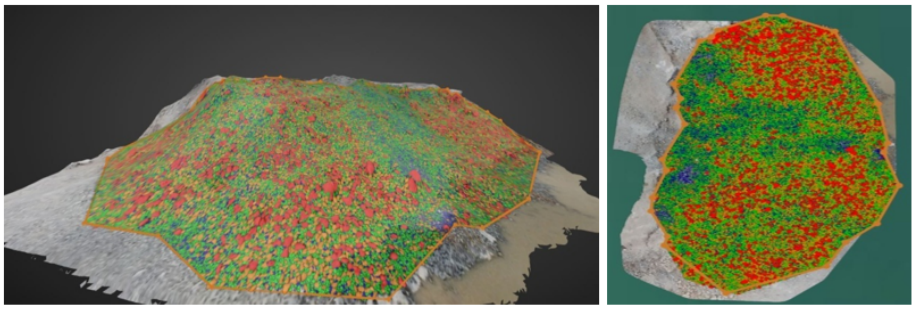

Figure 7. Rock fragmentation analysis in Strayos

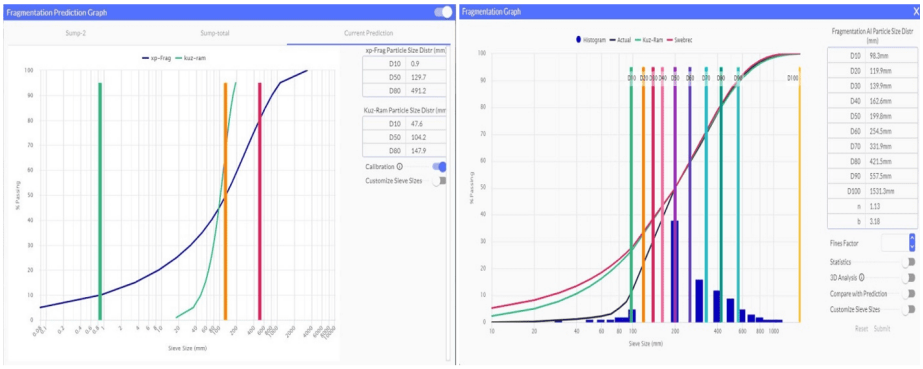

Figure 8. Prediction and actual fragmentation graphs

4 Machine Learning Approaches to Predict Rock Fragmentation

4.1 XGBoost Regression

XGBoost is an advanced solution based on gradient boosting decision trees, offering a scalable, portable, and distributed gradient boosting library [27–29]. This model effectively handles classification and regression tasks by generating boosted trees and operating in parallel [28]. Its core function involves optimizing the objective function value and constructing machine learning algorithms using gradient boosting. With its parallel tree boosting capability, XGBoost can efficiently and accurately address a wide range of engineering challenges.

$$\mathrm{Obj}(\theta) = \frac{1}{\mathrm{n}} \sum_{\mathrm{i}}^{\mathrm{n}} L(Yi - Yi) + \sum_{\mathrm{j}=1}^{\mathrm{j}} \Omega(\mathrm{fj}) \tag{1}$$

In the model, L represents the regularization term, which controls the complexity of the model to prevent overfitting and is used alongside the training loss function to evaluate performance on training data [30]. The prediction from the j-th tree is denoted by Yj and fj in the formula. Trees were constructed using the gradient (error term) and the Hessian, which is the second-order derivative of the loss. The loss at the current estimate is computed as follows:

$$\mathrm{h_m}(x) = \frac{\partial^2 L(Y, f(x))}{\partial f(x)^2} \tag{2}$$

where, $f(x)$ = $f(m-1)(x)$ and L is the loss of function.

$$\text{Similarity Score } = \frac{(\text{ Sumofresiduals })^2}{(N + \lambda)} \tag{3}$$

where, λ is $L2$ regularization term of weights.

Gain of the root node is as follows:

$$\text{Gain } = \text{ Left similarity } + \text{ Right similarity } - \text{ Root similarity} \tag{4}$$

$$\text{Output Value } = \frac{(\Sigma \text{ Residual i})}{\Sigma[\text{ Previous Probability i} \times (1 - \text{ Previous Probability i})] + \lambda} \tag{5}$$

4.2 PSO Algorithm

PSO has been applied across various fields, including geotechnical engineering and mining [31]. A hybrid approach combining PSO with ANNs has been used to estimate safety factors in the mining industry. Hasanipanah et al. [32] found that PSO effectively enhanced the performance of ANNs. Similarly, the integration of PSO with an Adaptive Neuro-Fuzzy Inference System (ANFIS) has been employed to predict blast fragmentation, demonstrating that PSO significantly improves ANFIS outcomes [33]. PSO highlights the success in predicting rock fragmentation [34].

In the PSO algorithm, initialization begins by generating a swarm of particles, where each particle represents a potential solution to the optimization problem. These particles are initialized with random positions and velocities within the search space, and each particle is assigned a fitness value based on the objective function being optimized. The performance of each particle is evaluated using this fitness value, which determines how close the particle's current position is to the optimal solution.

To assess particle performance and identify the best positions, the algorithm tracks two key metrics: the local and global best positions. The former refers to the best position a particle has achieved individually during its flight, while the latter is the best position found by any particle in the entire swarm. After each iteration, the particles update their velocities and positions based on both their personal best positions and the global best position, balancing exploration and exploitation in the search space. The algorithm continues to iterate until a stopping criterion is met, which could be a predefined number of iterations, a satisfactory fitness level, or a convergence of the swarm around a particular solution.

The PSO algorithm introduced is recognized as a reliable computational intelligence method. Inspired by the behaviour of social animals or particles, PSO addresses optimization challenges by representing each solution as a particle. The algorithm operates through several stages to find the optimal solution:

Step 1: After initializing the particle population and setting their velocities to zero, the ideal positions on both local and global scales are determined by assessing the particles' performance.

Step 2: Each particle moves within the search space at a specific velocity. To evaluate the effectiveness of the PSO-XGBoost models, the global best and local best are calculated for each iteration. The former represents the best position found across the entire search space, while the latter refers to the best position found within the current loop.

Step 3: After calculating the particles' velocities, their positions are updated based on the computed speeds within the search radius. The algorithm adjusts the new velocities of the particles using Eq. (6):

$$\mathrm{v_j^{i+1}} = \mathrm{wv_j^{(i)}} + \left(\mathrm{c_1} \times \mathrm{r_1} \times \left(\text{ local best j} - \mathrm{x_j^{((i)}}\right)\right) + \left(\mathrm{c_2} \times \mathrm{r_2} \times \left(\text{ global best j} - \mathrm{x_j^{(i)}}\right)\right), \mathrm{v_{min}} \tag{6}$$

where, $x_j^{(i)}$ represents particle j's position during iteration I; $v_j^{(i)}$ represents the particle velocity during iteration I; w denotes the inertial weight coefficient; I is the number of iterations; and $r1$ and $r2$ denote the numbers between $[0, 1]$.

As particles become more easily removable, both the local and global best positions can be updated. Using Eq. (7), the system was calculated, and then the updated position for each particle was determined as follows:

$$x_j{}^{i+1} = x_j{}^{(i)} + v_j{}^{(i+1)}; j = 1, 2, \ldots\ldots\ldots\ldots, n \tag{7}$$

The termination standards were then evaluated. Once the termination condition was satisfied, the global best solution was identified and established as the optimal solution to the problem.

5 Results and Discussion

A total of 137 blasts were conducted with varying explosive quantities, as detailed in Table 1. The data was divided, with approximately 80% allocated for training and the remaining 20% reserved for testing. The data not used for training was employed to test the model and evaluate its performance using RMSE and $\mathbf{R^2}$ metrics.

Table 1. Training and testing datasets of the model

Parameters	Mean		Median		Mode	
	Training	Testing	Training	Testing	Training	Testing
Spacing	8.13	8.10	8	8	8	8
Burden	6.2	6.3	6	6	6	6
S/B ratio	1.27	1.26	1.3	1.3	1.3	1.3
Total explosive quantity (kg)	6804	6199	7260	6210	8100	5940
Fragmentation (mm)	0.643	0.772	0.56	0.86	1	1

5.1 Implementation of the XGBoost-POS-T Algorithm

The integration of XGBoost with PSO and the Tri-Weight technique in the XGBoost-PSO-T model creates a robust and highly accurate predictive tool. XGBoost provides a strong baseline predictive model, while PSO enhances this by optimizing the hyperparameters more effectively than traditional grid search methods. The Tri-Weight technique further refines the model's predictions by reducing the impact of noise and outliers. The combined approach results in a model that not only achieves high accuracy but also generalizes well to unseen data, making it particularly useful in complex, high-dimensional problems where traditional methods may struggle.

In this study, the XGBoost algorithm was primarily used to estimate rock fragmentation. The effectiveness of the XGBoost model was adjusted using two key hyper-parameters, k and d. The PSO algorithm was employed to determine the optimal values for k and d. The PSO-XGBoost model was developed by utilizing a global search technique within PSO to find the best k and d values for the XGBoost model. The PSO-XGBoost approach was refined by splitting the data into training and testing sets (80% and 20%, respectively). To enhance the efficiency of XGBoost, the Tri-Weight kernel function, as described in Eq. (8), was implemented.

$$\text{Tri-weight: } K(u) = \frac{35}{32}\left(1 - u^2\right)^3 \tag{8}$$

In this study, k is a variable that can take non-negative values. The primary objective of using these kernel functions is to transform the data into a higher-dimensional space through linear mapping, which enhances the accuracy of fragmentation value regression in the modeling process. Details on kernel functions for XGBoost are discussed in the next stage.

The next phase involves optimizing XGBoost, assessing its performance, and verifying termination criteria to achieve optimal results. This phase aims to develop the most effective XGBoost model with minimal fitness value by finding the best hyper-parameters ($L1L1L1$ and $L2L2L2$) using the PSO algorithm. To ensure the XGBoost model's effectiveness with the PSO algorithm, RMSE and R^2 were used as the fitness function, as indicated in Eq. (9). Once the optimization process with the PSO algorithm is complete, the final predictive model for fragmentation is generated. The quality of this model was evaluated using the training dataset and performance metrics such as MAE, RMSE, and R^2.

The performance indicators are computed as follows:

$$\mathrm{RMSE} = \frac{1}{\mathrm{n}}\sum_{\mathrm{i}=1}^{\mathrm{n}}(yi - Yi)2 \tag{9}$$

where, n stands for the number of data points; yi stands for the observed values; and Yi stands for the anticipated values. MSE is, therefore, the average squared difference between the actual value and the value anticipated.

$$R^2 = 1 - \frac{\sum i(\widehat{yl} - \overline{y})\Big) 2}{\sum i(yi - \overline{y})2} \tag{10}$$

Here $\hat{y}$ represents the prediction or a point on the regression line, $\bar{y}$ represents the mean of all the values and yi represents the actual values or the points. This study highlights the performance of fragmentation predictive algorithms. Efficiency metrics for the XGBoost and XGBoost-PSO-T models were evaluated using RMSE and R^2, as detailed in Table 2. Figure 9 illustrates that the XGBoost-PSOT method provides a better fit compared to the standard XGBoost model. The XGBoost-PSO-T model achieved RMSE of 0.457 and R^2 of 0.951 on the training dataset, outperforming the standard XGBoost model, which achieved RMSE of 0.930 and R^2 of 0.822, as shown in Figure 10 and Figure 11. When assessing the model's performance on the testing dataset, the XGBoost-PSO-T algorithm also outperformed the other models, with RMSE of 0.657 and R^2 of 0.922. Additionally, histograms of explosive quantity and rock fragmentation are presented in Figure 12.

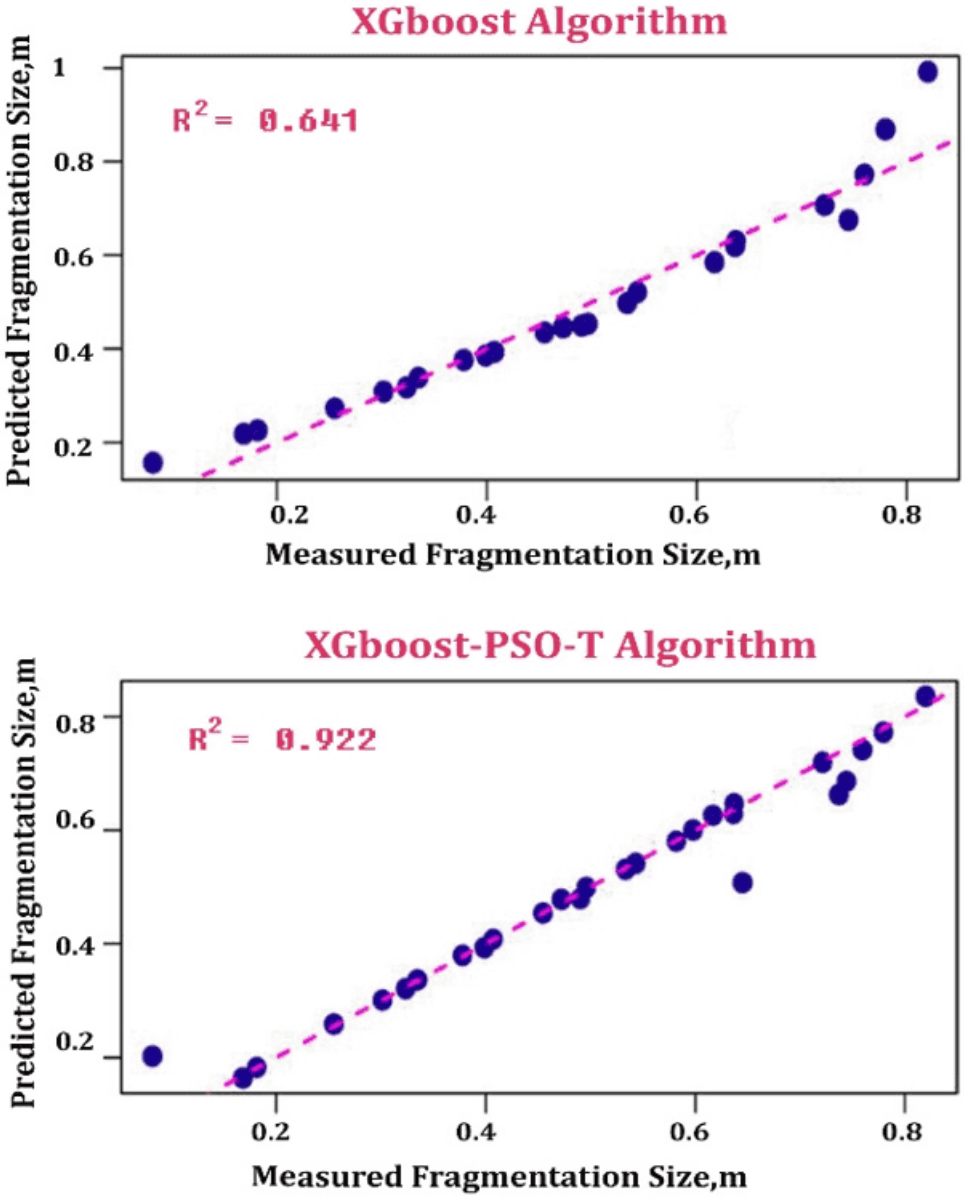

Figure 9. Fragmentation efficiency of measured VS. predicted values in XGBoost and XGBoost-PSO-T models

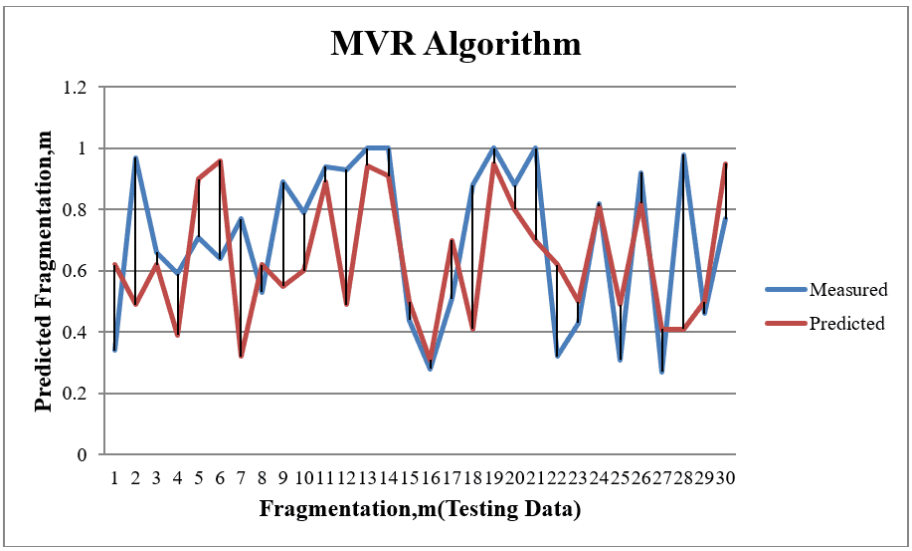

Figure 10. Fragmentation efficiency comparison between predicted and testing data sets using XGBoost

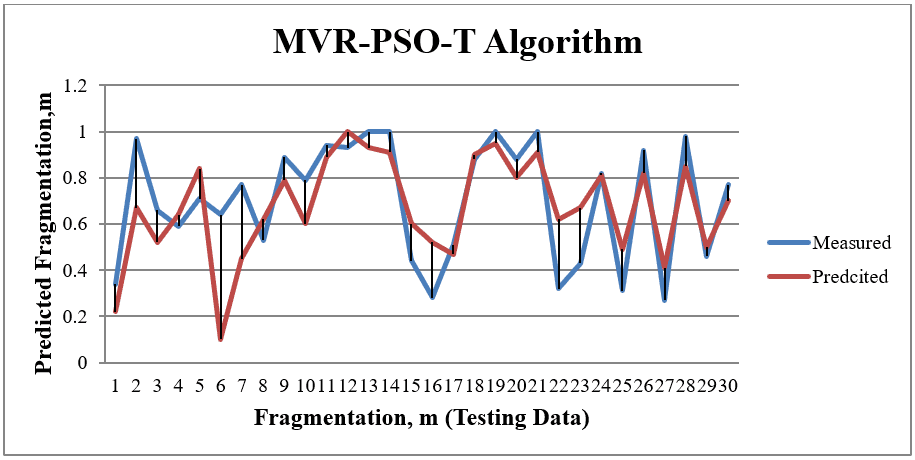

Figure 11. Fragmentation efficiency comparison between predicted and testing data sets using XGBoost and XGBoost-PSO-T models

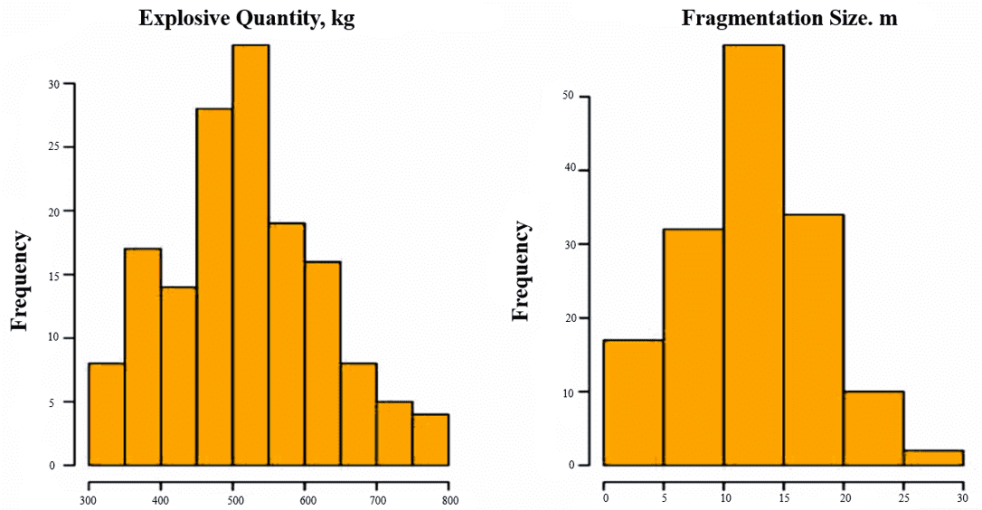

Figure 12. Histogram of rock fragmentation datasets

Table 2. Metric efficiency of models in predicting rock fragmentation

No.	Model	Training Data Set		Training Data Set	
		RMSE	R^2	RMSE	R^2
1	XGBoost	0.947	0.741	0.920	0.812
2	XGBoost-PSO-T	0.437	0.941	0.647	0.923

6 Conclusion

Minimizing rock fragmentation is a crucial objective, and extensive research is underway to find the most effective methods for reducing rock particle sizes to facilitate downstream operations and cut costs. The high accuracy of the XGBoost-PSO-T model demonstrated in this study suggests that AI techniques are promising solutions for this challenge.

• This study focuses on a single parameter, explosive quantity, to predict rock fragmentation and thoroughly assess its impact on fragmentation. A total of 152 blasts were conducted at the site with varying explosive quantities.

• The use of a Mavic Pro drone significantly improved the precision and clarity of muck pile photographs.

• AI-driven blasting software was instrumental in designing and analyzing rock fragmentation.

• The PSO algorithm proved to be an excellent tool for fine-tuning rock fragmentation estimates. According to RMSE and R^2 metrics, it significantly enhances the accuracy of the XGBoost algorithm, as detailed in Table 2. Although integrating PSO with XGBoost can be complex, it yields effective results.

• The proposed XGBoost-PSO-T model represents an innovative approach for predicting fragmentation and addressing other blasting challenges in practical engineering, offering a more advanced method for estimating rock fragmentation through bench blasting.

Data Availability

The data used to support the findings of this study are available from the corresponding author upon request.

Conflicts of Interest

The authors declare that they have no conflicts of interest.

References

[1] P. K. Singh, M. P. Roy, R. K. Paswan, Md. Sarim, S. Kumar, and R. Ranjan Jha, "Rock fragmentation control in opencast blasting," *J. Rock Mech. Geotech.*, vol. 8, no. 2, pp. 225–237, 2016. https://doi.org/10.1016/j.jrmge.2015.10.005

[2] F. Faramarzi, H. Mansouri, and M. A. Ebrahimi Farsangi, "A rock engineering systems based model to predict rock fragmentation by blasting," *Int. J. Rock Mech. Min. Sci.*, vol. 60, pp. 82–94, 2013. https://doi.org/10.1016/j.ijrmms.2012.12.045

[3] A. K Chakraborty, A. K Raina, M. Ramulu, P. B Choudhury, A. Haldar, P. Sahu, and C. Bandopadhyay, "Parametric study to develop guidelines for blast fragmentation improvement in jointed and massive formations," *Eng. Geol.*, vol. 73, pp. 105–116, 2004. https://doi.org/10.1016/j.enggeo.2003.12.003

[4] N. S. Chandrahas, B. S. Choudhary, and M. S. Venkataramayya, "Competitive algorithm to balance and predict blasting outcomes using measured field data sets," *Comput. Geosci.*, vol. 27, no. 6, pp. 1087–1110, 2023. https://doi.org/10.1007/s10596-023-10254-x

[5] M. Naresh, N. S. Chandrahas, G. P. Kumar, T. P. Kumar, and K. S. Kumar, "Harmonizing blasting efficiency: A case study on evaluation and optimization of fragmentation size and ground vibration," *J. Instit. Eng.*, vol. 2024, 2024. https://doi.org/10.1007/s40033-024-00730-8

[6] S. K. Kannavena, T. Pradeep, N. Sri Chandrahas, and D. U. V. D. Prasad, "Prediction of back break using sensitivity analysis and artificial neural networks," *J. Instit. Eng.*, 2024. https://doi.org/10.1007/s40033-024-00653-4

[7] N. S. Chandrahas, B. S. Choudhary, and M. S. Venkataramayya, "Firing pattern and spacing burden ratio selection in jointed overburden benches using unmanned aerial vehicle and artificial intelligence based tool," in *Proceedings of the Second International Conference on Emerging Trends in Engineering (ICETE 2023)*, 2023, pp. 1334–1358. https://doi.org/10.2991/978-94-6463-252-1_134

[8] D. Ramesh, N. S. Chandrahas, M. S. Venkatramayya, M. Naresh, P. Talari, D. U. V. D. Prasad, K. S. Kumar, and V. V. Kumar, "Effects of spacing-to-burden ratio and joint angle on rock fragmentation: An unmanned aerial vehicle and AI approach in overburden benches," *Acadlore Trans. Geosci.*, vol. 2, no. 3, pp. 155–166, 2023. https://doi.org/10.56578/atg020303

[9] N. Sri Chandrahas, Y. Fissha, B. S. Choudhary, B. Olamide Taiwo, M. S. Venkataramayya, and T. Adachi, "Experimental data – driven algorithm to predict muckpile characteristics in jointed overburden bench using unmanned aerial vehicle and AI tools," *Int. J. Min., Recla. Environ.*, vol. 38, no. 8, pp. 642–676, 2024. https://doi.org/10.1080/17480930.2024.2340876

[10] E. Hamdi and J. du Mouza, "A methodology for rock mass characterisation and classification to improve blast results," *Int. J. Rock Mech. Min. Sci.*, vol. 42, no. 2, pp. 177–194, 2005. https://doi.org/10.1016/j.ijrmms.2004.07.005

[11] W. Zohu, N. H. Maerz, J. Myers, and J. Linz, "Multivariate clustering analysis of discontinuity data: Implementations and applications," in *Proceedings of the 38th U.S. Rock Mechanics Symposium, Washington, D.C.*, 2001, pp. 861–868.

[12] A. K. Verma and T. N. Singh, "A neuro-fuzzy approach for prediction of longitudinal wave velocity," *Neural Comput. Applic.*, vol. 22, no. 7-8, pp. 1685–1693, 2012. https://doi.org/10.1007/s00521-012-0817-5

[13] Z. X. Zhang, Y. Qiao, L. Y. Chi, and D. F. Hou, "Experimental study of rock fragmentation under different stemming conditions in model blasting," *Int. J. Rock Mech. Min. Sci.*, vol. 143, p. 104797, 2021. https://doi.org/10.1016/j.ijrmms.2021.104797

[14] B. S. C. N. S. Chandrahas and K. K. Rao, "An investigation into the effects of rock mass properties on mean fragmentation," *Arch. Min. Sci.*, vol. 66, no. 4, pp. 561–578, 2023. https://doi.org/10.24425/ams.2021.139597

[15] M. Babaeian, M. Ataei, F. Sereshki, F. Sotoudeh, and S. Mohammadi, "A new framework for evaluation of rock fragmentation in open pit mines," *J. Rock Mech. Geotech. Eng.*, vol. 11, no. 2, pp. 325–336, 2019. https://doi.org/10.1016/j.jrmge.2018.11.006

[16] M. Monjezi, A. Bahrami, and A. Yazdian Varjani, "Simultaneous prediction of fragmentation and flyrock in blasting operation using artificial neural networks," *Mech. Min. Sci.*, vol. 47, no. 3, pp. 476–480, 2010. https://doi.org/10.1016/j.ijrmms.2009.09.008

[17] A. Nourian and H. Moomivand, "Development of a new model to predict uniformity index of fragment size distribution based on the blasthole parameters and blastability index," *J. Min. Sci.*, vol. 56, no. 1, pp. 47–58, 2020. https://doi.org/10.1134/s1062739120016478

[18] X. Shi, "Combined ANN Prediction Model for Rock Fragmentation Distribution due to Blasting," *J. Inf. Comput. Sci.*, vol. 10, no. 11, pp. 3511–3518, 2013. https://doi.org/10.12733/jics20101979

[19] J. Singh, A. K. Verma, H. Banka, T. N Singh, and S. Maheshwar, "A study of soft computing models for prediction of longitudinal wave velocity," *Arabian J. Geosci.*, vol. 9, no. 3, p. 224, 2016. https://doi.org/10.1007/s12517-015-2115-x

[20] K. Sayevand, H. Arab, and S. B. Golzar, "Development of imperialist competitive algorithm in predicting the particle size distribution after mine blasting," *Eng. Comput.*, vol. 34, no. 2, pp. 329–338, 2017. https://doi.org/10.1007/s00366-017-0543-9

[21] X. Z. Shi, J. Zhou, B. Wu, D. Huang, and W. Wei, "Support vector machines approach to mean particle size of rock fragmentation due to bench blasting prediction," *T. Nonferr. Metals Soc.*, vol. 22, no. 2, pp. 432–441, 2012. https://doi.org/10.1016/s1003-6326(11)61195-3

[22] K. Sayevand and H. Arab, "A fresh view on particle swarm optimization to develop a precise model for predicting rock fragmentation," *Eng. Computations*, vol. 36, no. 2, pp. 533–550, 2019. https://doi.org/10.1108/ec-06-2018-0253

[23] N. Sri Chandrahas, B. S. Choudhary, M. Vishnu Teja, M. S. Venkataramayya, and N. S. R. Krishna Prasad, "Xgboost algorithm to simultaneous prediction of rock fragmentation and induced ground vibration using unique blast data," *Appl. Sci.*, vol. 12, no. 10, p. 5269, 2022. https://doi.org/10.3390/app12105269

[24] T. Hudaverdi, H. S. W. Pinnaduwa, S. Kulatilake, and C. Kuzu, "Prediction of blast fragmentation using multivariate analysis procedures," *Int. J. Numer. Anal. Met.*, vol. 35, no. 12, pp. 1318–1333, 2010. https://doi.org/10.1002/nag.957

[25] J. M. Adebola, D. A. Ogbodo, and E. O. Peter, "Rock fragmentation prediction using Kuz-Ram model," *J. Environ. Earth Sci.*, vol. 6, no. 5, pp. 110–114, 2016.

[26] A. Karami and S. Afiuni-Zadeh, "Sizing of rock fragmentation modeling due to bench blasting using adaptive neuro-fuzzy inference system (ANFIS)," *Int. J. Min. Sci. Techno.*, vol. 23, no. 6, pp. 809–813, 2013. https://doi.org/10.1016/j.ijmst.2013.10.005

[27] M. Chen, Q. Liu, S. Chen, Y. Liu, C. H. Zhang, and R. Liu, "Xgboost-Based Algorithm Interpretation and Application on Post-Fault Transient Stability Status Prediction of Power System," *IEEE Access*, vol. 7, pp. 13 149–13 158, 2019. https://doi.org/10.1109/access.2019.2893448

[28] T. Chen and T. He. (2022) Xgboost: Extreme gradient boosting. https://cran.microsoft.com

[29] J. Friedman, T. Hastie, and R. Tibshirani, "Additive logistic regression: A statistical view of boosting (with discussion and a rejoinder by the authors)," *Annals Stati.*, vol. 28, pp. 337–407, 2000. http://doi.org/10.1214/

aos/1016218223

[30] J. H. Friedman, "Stochastic gradient boosting," *Comput. Stat. Data An.*, vol. 38, pp. 367–378, 2002. https://doi.org/10.1016/S0167-9473(01)00065-2

[31] M. Hasanipanah, D. Jahed Armaghani, H. Bakhshandeh Amnieh, M. Z. A. Majid, and M. M. D. Tahir, "Application of PSO to develop a powerful equation for prediction of flyrock due to blasting," *Neural Comput. Appl.*, vol. 28, no. S1, pp. 1043–1050, 2016. https://doi.org/10.1007/s00521-016-2434-1

[32] M. Hasanipanah, R. Naderi, J. Kashir, S. A. Noorani, and A. Z. A. Qaleh, "Prediction of blast-produced ground vibration using particle swarm optimization," *Eng. Comput.*, vol. 33, no. 2, pp. 173–179, 2016. https://doi.org/10.1007/s00366-016-0462-1

[33] B. Gordan, D. Jahed Armaghani, M. Hajihassani, and M. Monjezi, "Prediction of seismic slope stability through combination of particle swarm optimization and neural network," *Eng. Comput.*, vol. 32, no. 1, pp. 85–97, 2015. https://doi.org/10.1007/s00366-015-0400-7

[34] E. Ghasemi, H. Kalhori, and R. Bagherpour, "A new hybrid ANFIS–PSO model for prediction of peak particle velocity due to bench blasting," *Eng. Comput.*, vol. 32, no. 4, pp. 607–614, 2016. https://doi.org/10.1007/s00366-016-0438-1